Review

Exploring the Key Pathogenesis and Potential Intervention Targets of Sulforaphane in Acute Kidney Injury in Sepsis Based on Bioinformatics

Fengqi Liu[1], Kankai Tang[1], Peifeng Zhu[2]*

[1]Department of Intensive Care Unit, the First Affiliated Hospital of Huzhou University, Huzhou, China
[2]Department of General Surgery, the First Affiliated Hospital of Huzhou University, Huzhou, China

Keywords. Sepsis; Acute kidney injury; Sulforaphane; *FKBP1A*; NF-κB signaling pathway; Public chip database; Bioinformatics

Introduction. The objective was to use bioinformatics to analyze the potential key genes involved in the mechanism of sulforaphane's protective effects in sepsis-associated acute kidney injury (SA-AKI) and to identify potential intervention targets.
Methods. Gene Expression Omnibus (GEO) gene chip datasets containing gene expression profiles from kidney tissues of SA-AKI patients and normal controls were selected. Upregulated differentially expressed genes (DEGs) were identified using GEO2R. Protein-protein interaction (PPI), GO, and KEGG enrichment analyses were performed. Allyl isothiocyanate's target genes were analyzed in the ChEMBL database, and intersections with the above DEGs were presented in Venn diagrams. Rat tissues were examined for FKBP1A expression using qRT-PCR.
Results. A total of 17 DEGs related to SA-AKI were obtained (|log fold change| > 0 and $P < .05$). KEGG pathway analysis indicated that the primary pathways linked to the elevated DEGs were glycogen breakdown, leukocyte trans-endothelial migration, and T-cell receptor, TNF, and NF-κB signaling. The module and PPI network analysis of common DEGs revealed one cluster and four candidate genes, including *OASL*, *TRRAP*, *FKBP1A*, and *BANF*. ChEMBL database analysis identified 339 target genes for allyl isothiocyanate, and the intersection with upregulated DEGs related to SA-AKI injury yielded two co-expressed genes, *FKBP1A* and *TRRAP*. According to the findings of the qRT-PCR assay, the kidney tissues of the model cohort showed significantly higher expression levels of FKBP1A mRNA than the control cohort ($P = .0142$).
Conclusion. Allyl isothiocyanate may alleviate SA-AKI injury by targeting FKBP1/NF-κB.

IJKD 2024;18:245-54
www.ijkd.org
DOI: 10.52547/ijkd.8075

INTRODUCTION

Sepsis is the dysregulated inflammatory body response to various infections, causing life-threatening multi-organ dysfunction.[1] The defining characteristic is the rapid onset of an inflammatory response, leading to the production of several inflammatory cytokines, such as TNF-α, IL-8, IL-6, and IL-1β, which subsequently activates the host's immune system.[2] This is associated with activation of the sympathetic nervous system, vasoactive substance production, endothelial damage, oxidative stress injury, and cell apoptosis, with oxidative stress injury being a crucial link.[3] These factors can damage renal tissues through

complex molecular mechanisms, triggering acute kidney injury (AKI). Currently, sepsis is a major cause of AKI, accounting for between 45 and 70% of all cases.[4] A prospective survey on the epidemiology of AKI worldwide revealed that over half of critically ill patients experience AKI, with approximately 47% attributed to sepsis.[5]

Currently, no specific regimen is available to treat sepsis-associated AKI (SA-AKI), and SA-AKI-related mortality remains exceptionally high.[6] Some medications for treating sepsis are selected based on the characteristics of sepsis occurrence, including those extracted from plant species. Sulforaphane, an organosulfur molecule derived from cruciferous plants, has exhibited multiple biological actions, including anticancer, antioxidant, antiplatelet activation, anti-inflammatory, and detoxifying properties.[7] Research indicates that suppressing the production of reactive nitrogen and reactive oxygen species (ROS) is advantageous for mitigating oxidative damage and the severity of AKI, thereby decreasing the mortality rate.[8]

This study hypothesized that sulforaphane can alleviate the severity of SA-AKI by modulating oxidative stress pathways and inflammatory responses. Sulforaphane target-specific genes critically involved in these pathways were predicted, thus offering a therapeutic advantage in managing SA-AKI. The current study was designed to identify and analyze differentially expressed genes (DEGs) in SA-AKI using bioinformatics, revealing disease-related signaling pathways, and investigate the interaction between sulforaphane and target genes in SA-AKI. Finally, the bioinformatics prediction was experimentally verified using an *in-vivo* rat model to evaluate whether sulforaphane could effectively regulate gene expression and improve SA-AKI symptoms.

STUDY METHODOLOGY

Data source

Gene chip datasets (GSE12624 and GSE116849) comprising SA-AKI damage and normal control groups were obtained from the Gene Expression Omnibus (GEO) database (https://www.ncbi.nlm.nih.gov/geo). The criteria for dataset inclusion were: (1) the selected datasets must be whole-genome expression mRNA chip data, (2) the data should include the SA-AKI injury group and normal control group, and (3) the original datasets must undergo standardized processing.

Data processing and DEG selection

Using the GEO2R web application in GEO, differentially expressed genes (DEGs) were investigated using the criteria $|\log \text{fold change}| > 0$ and $P < .05$. The shared DEGs from the two chips included genes with inconsistent upregulation and downregulation. The shared DEGs were identified using Venn diagrams, and DEG-associated pathways were examined using bioinformatics. Only upregulated DEGs were analyzed to prevent the influence of potentially co-expressed genes and false positives, and to identify possible clinical targets. Heatmaps and volcano plots of the DEGs were created using R. The upregulated DEGs shared between the datasets were identified by Venn diagrams to determine consistently upregulated DEGs linked to SA-AKI.

GSEA, GO, and KEGG analyses

The functions of the SA-AKI-associated DEGs were investigated using GO and KEGG enrichment analyses. DEGs enriched in the GO categories of biological process (BP), cellular component (CC), and molecular function (MF). Gene Set Enrichment Analysis (GSEA) was performed to determine DEG-associated pathways.

Protein-protein interaction (PPI) analysis of shared DEGs

The PPI network of the shared DEGs was constructed using STRING (https://string-db.org/), using Cytoscape to import the results and do correlation analysis and visualization. The Molecular Complex Detection (MCODE) plugin uses protein complex clustering techniques to eliminate important protein expression molecules.

Exploration of sulforaphane's target genes in the ChEMBL database

The ChEMBL database (https://www.ebi.ac.uk/chembl/) was utilized to extract sulforaphane from the webpage, identify corresponding compounds, and examine and obtain the relevant target genes.

Construction of AKI rat model

Twenty SPF-grade, healthy male Eight-week-old Sprague-Dawley rats were kept in a climate-controlled chamber with a 22°C ± 2°C temperature

regulation and a light-dark cycle. Food and water were freely available to the rats. The study received approval from the Animal Ethics Committee of the First Affiliated Hospital of Huzhou University. Ten rats were placed in the control and model groups, which were randomly formed. The traditional method of cecal ligation and puncture was employed to develop the SA-AKI rat model. A 2% pentobarbital sodium injection (of 20 mg/kg)) was used to anaesthetize the rats. A midline abdominal incision of approximately 1 cm was made after exposing the cecum. The cecum was ligated at its base, and three punctures were made with a 2.6 mm-triangular needle. Following the expulsion of only a small amount of faeces, the intestine was repositioned, and the abdominal cavity was sutured in layers. The control group underwent cecal exploration without ligation and puncture.

Hematoxylin and eosin (H&E) staining of renal tissues

Samples of rat kidneys were extracted under sterile conditions at 24 hrs after cecal ligation and puncture, then fixed in 4% paraformaldehyde (Sigma-Aldrich, USA) for 72 hrs, dehydrated in an ethanol gradient, cleared with xylene, paraffin-embedded, and sectioned. Following deparaffinization and rehydration in phosphate buffer saline (PBS), the slices were stained with hematoxylin for 10 minutes, differentiated in 0.7% HCl acid alcohol, counterstained with eosin for 3 minutes after rinsing, dehydrated in an ethanol gradient, cleared with xylene, and ultimately mounted with neutral gum. The H&E staining kit (C0105S) was obtained from Shanghai Biyuntian Biotechnology Co., Ltd. The slides were examined and analyzed using a light microscope.

qRT-PCR

TRIzol (Thermo Fisher, USA) was used to extract total RNA from rat kidney tissues. RNA was reverse transcribed into cDNA utilizing a ReverAid First Strand cDNA Synthesis Kit (Takara, Japan) with 1 µg of RNA. The cDNA was amplified by qRT-PCR utilizing SYBR Green Mixture (Takara). The target gene expression was normalized to GAPDH. The primer sequences were as follows:

- *FKBP1A* forward:
5′-CCTCCGGGACAGAAACAAG-3′
- *FKBP1A* reverse:
5′-TGTCGGAAGCAAAGCTGAGT-3′
- GAPDH forward:
5′-GAGGGACCCAGCCAACATTA-3′
- GAPDH reverse:
5′-TGACAAACATGGGGGCATCT-3′

Statistical analysis

GraphPad Prism software (version 7.0) was applied to perform the data visualization and statistical analysis. All data are expressed as mean ± standard deviation (SD). T-tests were employed in the DEG analysis to ascertain p-values and p-values modified by false discovery rate (FDR). *P*-values < .05 signify statistically significant variations.

RESULTS

Screening of DEGs related to SA-AKI DEGs associated with SA-AKI injury were identified by evaluating gene chip datasets from the GEO database (GSE12624 and GSE116849). The data was visualized using sample-normalized box graphs and volcano plots for DEGs (Figures 1A and 1B). The focus was on upregulated DEGs, with 1007 upregulated DEGs identified in GSE12624 and 429 in GSE116849. Upregulated DEGs shared between the two datasets were identified by Venn diagrams, which revealed 17 genes associated with SA-AKI injury (Figure 1C, Table 1).

KEGG and GO enrichment analysis

Enrichment analysis was performed utilizing the DAVID online database on the observed shared differentially expressed genes, with a baseline set as *Homo sapiens*. The enhanced data concerning GO indicated that the upregulated DEGs participated in multiple biological processes, including regulating the leucine-sensitive calcium release channel activity, the positive modulation

Table 1. Upregulated DEGs shared by the GSE12624 and GSE116849 datasets

VPS45	PAK3	TOMM70A	BANF1	OASL
TNRC6A	RIC8B	VCAM1	GPR3	PCOLCE
CCDC132	SRI	M6PR	MAN2B2	TRRAP
MOBP	FKBP1A			

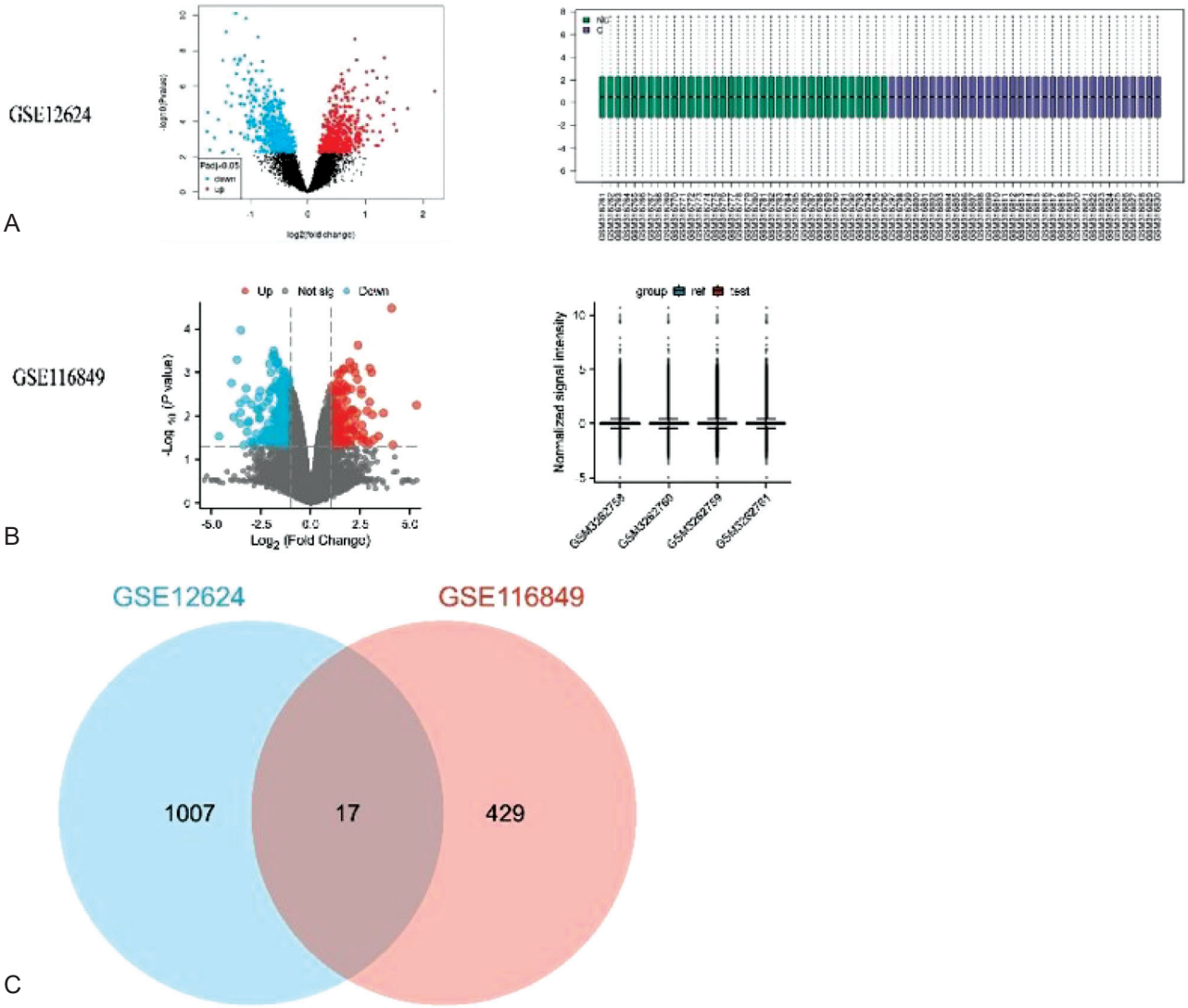

Figure 1. Screening of DEGs in SA-AKI. (A) Volcano plot and sample normalized box plot of DEGs in the GSE12624 dataset; (B) The sample-normalized box plot and Volcano plot of DEGs in the GSE116849 dataset; (C) Venn diagram for DEGs that are overexpressed in GSE12624 and GSE116849. DEGs, differentially expressed genes; SA-AKI, sepsis-associated acute kidney injury.

of cAMP-mediated signaling, the regulation of the RIG-I signaling pathway, the negative regulation of transcription regulatory region DNA binding, histone H2A acetylation, the negative regulation of protein phosphatase activity, and the regulation of the activin receptor signaling pathway, etc. (Figure 2A). Regarding CCs, the DEGs were more abundant in structures such as the RISC complex, T-tubule, NuA4 histone acetyltransferase complex, myofibril, SAGA complex, H4/H2A histone acetyltransferase complex, and sarcoplasmic reticulum (Figure 2B). The investigation revealed correlations between MFs and the following: binding of transmembrane transporter proteins, binding of FK506, binding of α-mannosidase, binding of MAP kinase, binding of transforming growth factor beta receptor, binding of calcium channel regulator, and binding of peptidase activator (Figure 2C). According to the KEGG pathway analysis, the overexpressed DEGs were mainly linked to the pathways involved in glycogen degradation and leukocyte transendothelial migration, as well as T cell receptor, TNF, NF-κB, and ErbB signaling (Table 2 and Figure 2D).

Development of PPI network, module analysis, and core gene selection for common DEGs

A PPI network of the shared DEGs was constructed STRING. After that, the data were loaded into Cytoscape to examine and filter the protein interaction network visually. The Cytoscape Network Analyzer

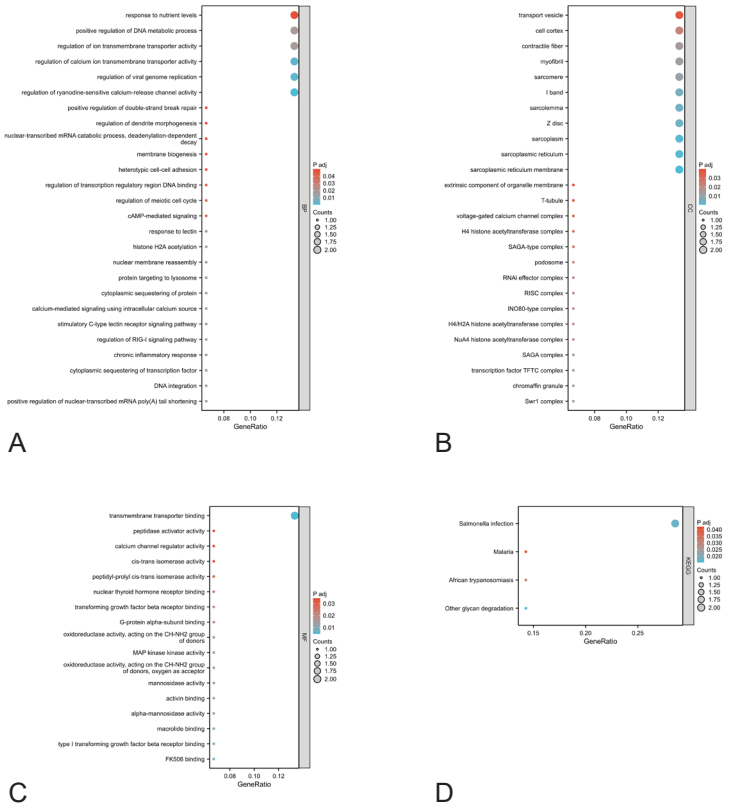

Figure 2. GO and KEGG enrichment analyses of DEGs. DEGs enriched in GO categories of biological process (A), cellular component (B), and molecular function (C); KEGG pathways with significant DEG enrichment (D).

Table 2. Top five findings of GO and KEGG enrichment analyses

Ontology	ID	Description	GeneRatio	BgRatio	*P*	P.adjust
BP	GO:0060314	control of the activity of calcium release channels responsive to ryanodine	2/15	26/18800	.0002	0.0002
BP	GO:0045071	inhibition of viral genome replication	2/15	57/18800	.0009	0.0009
BP	GO:0051279	regulation of the release of trapped calcium ions into the cytosol	2/15	80/18800	.0018	0.0018
BP	GO:0045069	regulation of viral genome replication	2/15	87/18800	.0021	0.0021
BP	GO:0048525	negative regulation of the viral process	2/15	91/18800	.0023	0.0023
CC	GO:0033017	sarcoplasmic reticulum membrane	2/15	41/19594	.0004	0.0004
CC	GO:0016529	sarcoplasmic reticulum	2/15	71/19594	.0013	0.0013
CC	GO:0016528	sarcoplasm	2/15	78/19594	.0016	0.0016
CC	GO:0030018	Z disc	2/15	127/19594	.0041	0.0041
CC	GO:0042383	sarcolemma	2/15	131/19594	.0044	0.0044
MF	GO:0044325	transmembrane transporter binding	2/15	127/18410	.0047	0.0047
MF	GO:0005528	FK506 binding	1/15	10/18410	.0081	0.0081
MF	GO:0034713	type I transforming growth factor beta receptor binding	1/15	10/18410	.0081	0.0081
MF	GO:0005527	macrolide binding	1/15	12/18410	.0097	0.0097
MF	GO:0004559	alpha-mannosidase activity	1/15	15/18410	.0122	0.0122
KEGG	hsa00511	Other glycan degradation	1/7	18/8164	.0153	0.0153
KEGG	hsa05132	Salmonella infection	2/7	249/8164	.0176	0.0176
KEGG	hsa05143	African trypanosomiasis	1/7	37/8164	.0313	0.0313
KEGG	hsa05144	Malaria	1/7	50/8164	.0421	0.0421
KEGG	hsa05211	Renal cell carcinoma	1/7	69/8164	.0577	0.0577

GO, Gene Ontology; KEGG, Kyoto Encyclopedia of Genes and Genomes; BP, biological process; CC, cellular component; MF, molecular function.

tool was employed for the undirected assessment of each node in the PPI network, determining the degree values for individual nodes. The node's size indicated the degree value, the neighborhood's degree of connectivity was indicated by the node's color changing from red to green, and the total score value was shown by the thickness of the edges. All protein nodes were arranged using the attribute circle pattern, with nodes of 4 degrees and higher located in the inner layer (Figure 3A). Clustering of these key proteins was performed with the MCODE plugin. The standard parameters were a value of 0.2 for node score threshold, 2 for the K-core value, and 100 as the maximum depth. This analysis revealed one high-scoring cluster (Figure 3B), identifying candidate key genes as *OASL*, *TRRAP*, *FKBP1A*, and *BANF1*.

Exploration of sulforaphane target genes in the ChEMBL database

The target genes of sulforaphane in the ChEMBL database were explored. A total of 339 target genes were obtained, and then a Venn diagram was established to intersect with the above 17 upregulated differential genes related to SA-AKI. Finally, two co-expressed genes were obtained, CHEMBL2095194 and CHEMBL2169736, and the corresponding genes were queried in the ChEMBL database as *FKBP1A* and TRRAP (Figure 4).

Construction of a rat model of AKI

The renal tubular epithelial cells in kidney tissue samples from control rats were observed to be intact and neatly organized, as demonstrated by H&E staining (C0105S). Compare to the control group, the model group showed glomerular hypertrophy with enlarged glomerular spaces, and the tubular epithelial cells were irregular in shape. Shedding, apparent dilation of the renal tubules, and vacuolar degeneration of the renal tubules indicated that the modeling was successful (Figure 5).

qRT-PCR to identify FKBP1A expression in rat tissues

qRT-PCR was used to measure the levels of FKBP1A mRNA in the tissues of both groups.

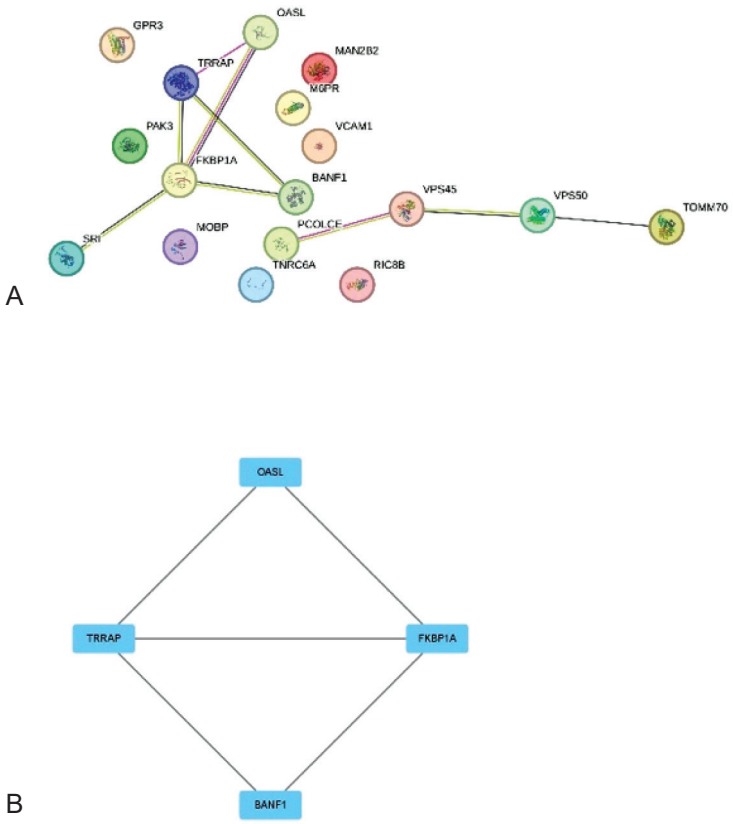

Figure 3. Venn diagram showing possible genes and the network of protein interactions. Diagram of protein interactions; (A) Cluster1; (B).

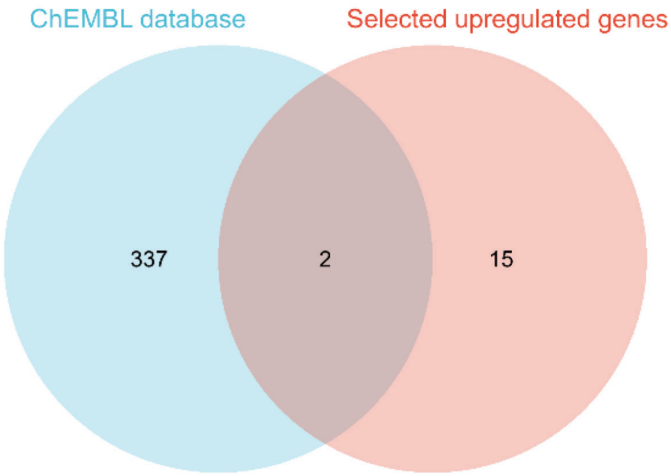

Figure 4. Venn diagram of differentially upregulated genes related to sulforaphane target genes and septic-associated acute kidney injury in ChEMBL database.

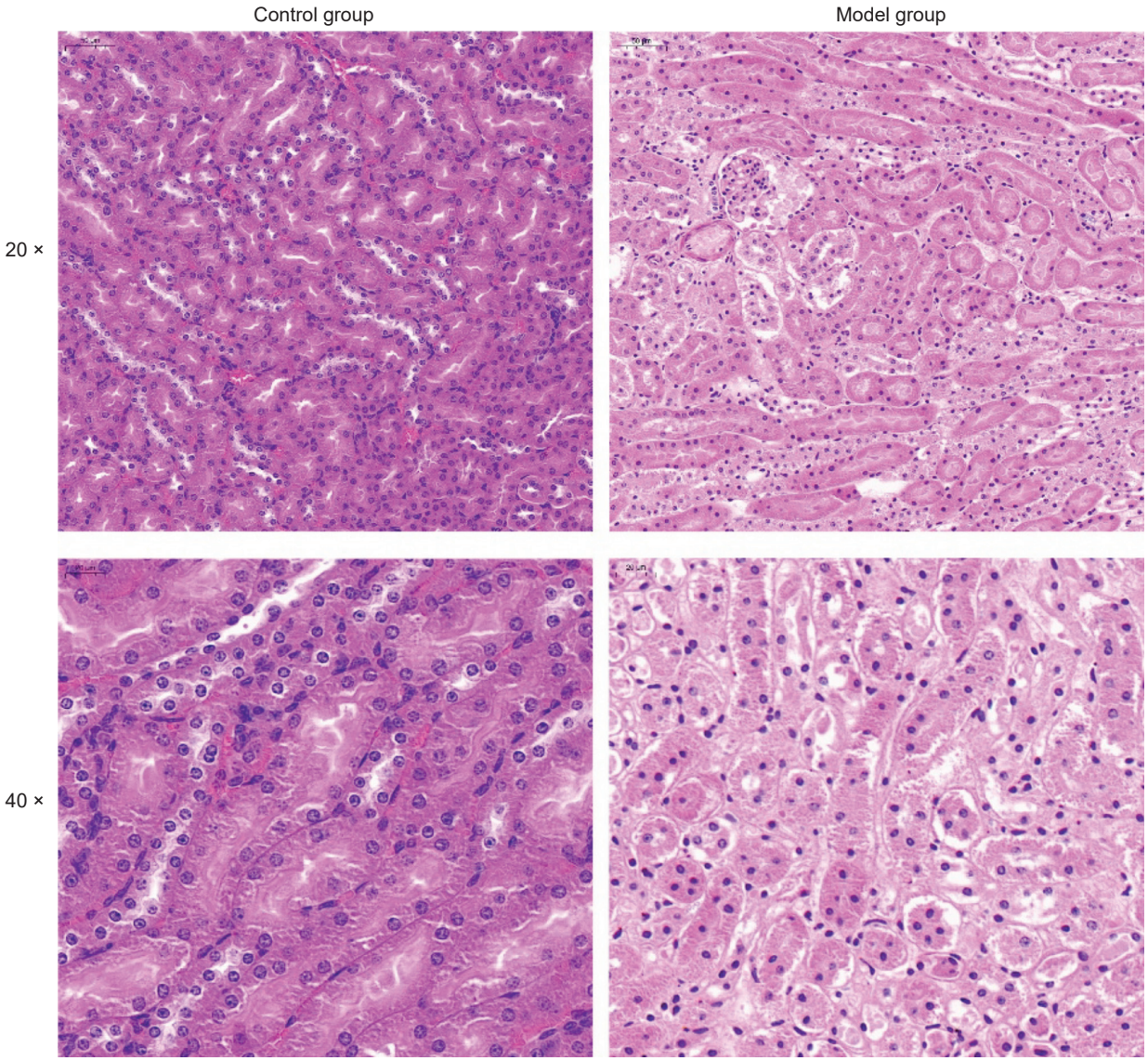

Figure 5. Kidney histological observation (H&E staining)

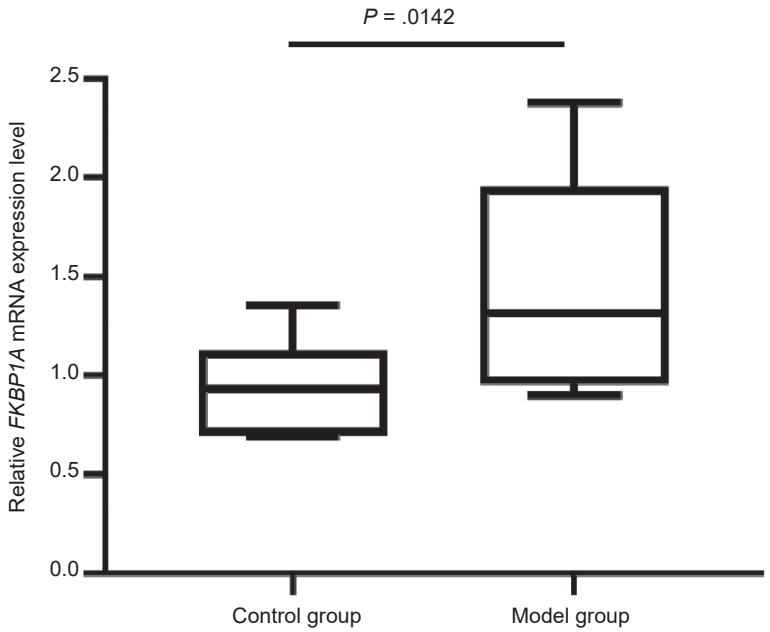

Figure 6. qRT-PCR detection of FKBP1A mRNA expression levels in rat tissues of 20 samples.

Relative to the controls, tissues in the model group showed higher FKBP1A expression (P = .0142, Figure 6).

DISCUSSION

The sulforaphane compound has garnered widespread attention owing to its multiple biological activities and pharmacological values. Various investigations have validated that the sulforaphane molecule exhibits diverse biological properties, encompassing anti-inflammatory, antioxidant, and immunomodulatory capabilities. As a result, it exhibits protective effects against multiple diseases, including malignancies, neurodegenerative disorders, cardiovascular diseases, obesity, and asthma.[9-12] Further research indicated that the sulforaphane compound primarily exerts its antioxidant ability by activating Nrf2. The activation results in the translocation of Nrf2 towards the nucleus, which associates with antioxidant response elements, thereby enhancing the production of phase II detoxifying enzymes.[13]

Conversely, in Nrf2 gene knockout mice, the sulforaphane compound lost its inherent antioxidant effect.[14] Therefore, the sulforaphane compound is currently considered a natural activator of Nrf2. Bao *et al.*[15] demonstrated that the sulforaphane compound alleviated oxidative stress damage induced by 1-methyl-4-phenylpyridinium in rat pheochromocytoma cells (PC12 cells) by activating the Nrf2-ARE axis. It has been found that the sulforaphane compound significantly reduced oxidative stress damage in lung tissues of septic rats with acute lung injury.[16]

Gene chips have recently gained broad implementation in disease research.[17] In the present study, 17 upregulated common DEGs were identified through bioinformatics analysis by searching the GEO database for datasets related to SA-AKI. The enriched KEGG pathways were mainly associated with glycogen degradation, ErbB signaling, and leukocyte trans-endothelial migration, as well as T-cell receptor, TNF, and NF-κB signaling. These pathways are crucial in inflammatory responses and immune regulation. The NF-κB axis has been reported to influence SA-AKI through proteins such as BAP1, a deubiquitinase that regulates BRCA1 protein stability and blocks NF-κB signaling in mouse models with sepsis-induced AKI.[18]

Additionally, puerarin alleviates lipopolysaccharide-induced AKI in mouse models by regulating the SIRT1/NF-κB axis.[19] MiR-22 lowers the injury caused by SA-AKI by blocking the HMGB1/TLR4/NF-κB axis.[20] The abovementioned investigations indirectly validate the current study's findings, indicating that the DEGs found here may be essential players in SA-AKI through modulating various signaling pathways. In developing the PPI

network and module analyzing the shared DEGs, 4 potential genes (*OASL*, *TRRAP*, *FKBP1A*, and *BANF1*) and one cluster were found. In the ChEMBL database, an intersection between the sulforaphane compound's target genes and those mentioned above, 17 upregulated DEGs related to SA-AKI were performed. The common differential genes were found to be *FKBP1A* and TRRAP. Although no direct research has been conducted on these genes in SA-AKI, previous studies suggested their potential relevance. For example, gene expression and cell apoptosis are regulated by the interaction of the transcription factor FoxO3 with the TRRAP subunit of the histone acetyltransferase complex.[21] When treated with oxidized low-density lipoprotein, dendrobine, which involves FKBP1, can prevent oxidative stress, inflammation, cell apoptosis, and aging in human umbilical vein endothelial cells.[22] This investigation hypothesized that sulforaphane compound might alleviate oxidative stress injury in SA-AKI by targeting FKBP1, potentially influencing the NF-κB signaling pathway. Further exploration and validation through relevant in *vitro* experiments are warranted.

Rats in the SA-AKI model group in our study had considerably greater levels of FKBP1A mRNA expression than rats in the control group. This finding indicates that FKBP1A may be crucial in the pathophysiology of SA-AKI. Its upregulation in the inflammatory response and cellular stress response induced by sepsis may represent a stress-protective reaction that helps maintain cell survival and function. The increased expression of FKBP1A underscores its potential regulatory role under pathological conditions and provides possibilities for drug targeting of this molecule. Considering that sulforaphane might exert protective effects by regulating such key molecules, future research could explore the efficacy of sulforaphane in preventing or alleviating SA-AKI and its specific mechanisms of action.

The present research has limitations, particularly the absence of pertinent in vivo investigations and validation through clinical data. Additional multicenter, large-sample size, future studies are necessary to validate and investigate the pertinent research findings.

CONCLUSION

Multifactorial regulation may be present in the process of SA-AKI. Identifying key genes and associated signaling networks helps enhance comprehension of their biological mechanisms. Moreover, sulforaphane has been identified as a potential mitigator of sepsis-induced acute kidney injury through its influence on the FKBP1/NF-κB pathway.

ACKNOWLEDGEMENT

N/A.

ETHICAL CONSIDERATIONS

The study received approval from the Animal Ethics Committee of the First Affiliated Hospital of Huzhou University.

CONFLICT OF INTEREST

The authors have no conflicts of interest to declare.

FUNDING

The study was supported by grants from the public welfare technology application research program of Huzhou (Grant no. 2021GYB49) and the medical and health research project of Zhejiang province (Grant no. 2021KY1094).

REFERENCES

1. Jia HM, Jiang YJ, Zheng X, et al. The attributable mortality of sepsis for acute kidney injury: a propensity-matched analysis based on multicenter prospective cohort study. Ren Fail. 2023;45(1):2162415. doi:10.1080/088602 2X.2022.2162415
2. Chen S, Kuang M, Qu Y, et al. Expression of Serum Cytokines Profile in Neonatal Sepsis. Infect Drug Resist. 2022;15:3437-3445. doi: 10.2147/IDR.S368772.
3. Singer M, Deutschman CS, Seymour CW, et al. The Third International Consensus Definitions for Sepsis and Septic Shock (Sepsis-3). JAMA. 2016;315(8):801-810. doi:10.1001/jama.2016.0287
4. Uchino S, Kellum JA, Bellomo R, et al. Acute renal failure in critically ill patients: a multinational, multicenter study. JAMA. 2005;294(7):813-818. doi:10.1001/jama.294.7.813
5. Hoste EA, Bagshaw SM, Bellomo R, et al. Epidemiology of acute kidney injury in critically ill patients: the multinational AKI-EPI study. Intensive Care Med. 2015;41(8):1411-1423. doi:10.1007/s00134-015-3934-7
6. Meersch M, Küllmar M, Schmidt C, et al. Long-Term Clinical Outcomes after Early Initiation of RRT in Critically Ill Patients with AKI. J Am Soc Nephrol. 2018;29(3):1011-1019. doi:10.1681/ASN.2017060694
7. Jiang X, Liu Y, Ma L, et al. Chemopreventive activity of sulforaphane. Drug Des Devel Ther. 2018;12:2905-2913. Published 2018 Sep 11. doi:10.2147/DDDT.S100534

8. Dennis JM, Witting PK. Protective Role for Antioxidants in Acute Kidney Disease. Nutrients. 2017;9(7):718. Published 2017 Jul 7. doi:10.3390/nu9070718
9. Basak P, Sadhukhan P, Sarkar P, Sil PC. Perspectives of the Nrf-2 signaling pathway in cancer progression and therapy. Toxicol Rep. 2017;4:306-318. Published 2017 Jun 13. doi:10.1016/j.toxrep.2017.06.002
10. Liu P, Atkinson SJ, Akbareian SE, et al. Sulforaphane exerts anti-angiogenesis effects against hepatocellular carcinoma through inhibition of STAT3/HIF-1α/VEGF signalling. Sci Rep. 2017;7(1):12651. Published 2017 Oct 4. doi:10.1038/s41598-017-12855-w
11. Ranaweera SS, Dissanayake CY, Natraj P, Lee YJ, Han CH. Anti-inflammatory effect of sulforaphane on LPS-stimulated RAW 264.7 cells and ob/ob mice. J Vet Sci. 2020;21(6):e91. doi:10.4142/jvs.2020.21.e91
12. Pearson BL, Simon JM, McCoy ES, Salazar G, Fragola G, Zylka MJ. Identification of chemicals that mimic transcriptional changes associated with autism, brain aging and neurodegeneration. Nat Commun. 2016;7:11173. Published 2016 Mar 31. doi:10.1038/ncomms11173
13. Wu W, Peng G, Yang F, Zhang Y, Mu Z, Han X. Sulforaphane has a therapeutic effect in an atopic dermatitis murine model and activates the Nrf2/HO-1 axis. Mol Med Rep. 2019;20(2):1761-1771. doi:10.3892/mmr.2019.10405
14. Oh CJ, Kim JY, Min AK, et al. Sulforaphane attenuates hepatic fibrosis via NF-E2-related factor 2-mediated inhibition of transforming growth factor-β/Smad signaling. Free Radic Biol Med. 2012;52(3):671-682. doi:10.1016/j.freeradbiomed.2011.11.012
15. Bao B, Zhang MQ, Chen ZY, et al. Sulforaphane prevents PC12 cells from oxidative damage via the Nrf2 pathway. Mol Med Rep. 2019;19(6):4890-4896. doi:10.3892/mmr.2019.10148
16. Zhao B, Gao W, Gao X, et al. Sulforaphane attenuates acute lung injury by inhibiting oxidative stress via Nrf2/HO-1 pathway in a rat sepsis model. Int J Clin Exp Pathol. 2017;10(8):9021-9028. Published 2017 Aug 1.
17. Tang Y, Yang X, Shu H, et al. Bioinformatic analysis identifies potential biomarkers and therapeutic targets of septic-shock-associated acute kidney injury. Hereditas. 2021;158(1):13. Published 2021 Apr 16. doi:10.1186/s41065-021-00176-y
18. Luo S, Gong J, Zhao S, Li M, Li R. Deubiquitinase BAP1 regulates stability of BRCA1 protein and inactivates the NF-κB signaling to protect mice from sepsis-induced acute kidney injury. Chem Biol Interact. 2023;382:110621. doi:10.1016/j.cbi.2023.110621
19. Guo J, Zhang W, Liang P, et al. Nan Fang Yi Ke Da Xue Xue Bao. 2023;43(7):1248-1253. doi:10.12122/j.issn.1673-4254.2023.07.22
20. Zhang J, Chen Q, Dai Z, Pan H. miR-22 alleviates sepsis-induced acute kidney injury via targeting the HMGB1/TLR4/NF-κB signaling pathway. Int Urol Nephrol. 2023;55(2):409-421. doi:10.1007/s11255-022-03321-2
21. Fusi L, Paudel R, Meder K, et al. Interaction of transcription factor FoxO3 with histone acetyltransferase complex subunit TRRAP modulates gene expression and apoptosis. J Biol Chem. 2022;298(3):101714. doi:10.1016/j.jbc.2022.101714
22. Lou D, Xing X, Liang Y. Dendrobine modulates autophagy to alleviate ox-LDL-induced oxidative stress and senescence in HUVECs. Drug Dev Res. 2022;83(5):1125-1137. doi:10.1002/ddr.21937

*Correspondence to:
Peifeng Zhu
Department of General Surgery, the First Affiliated Hospital of Huzhou University, Huzhou, China.
E-mail: dr_zpf@163.com

Received December 2023
Accepted April 2024